ARTICLE

π-Conjugated Unit-Dependent Optical Properties of Linear Conjugated Oligomers

Ning Sui[a,d], Lu Zou[a], Yun-fei Song[e*], Qiu-lin Zhong[a], Ying-hui Wang[a,c*], Xiao-gang Wei[b], Zeng-bin Wang[b], Yu-guang Ma[b], Yan-qiang Yang[d], Han-zhuang Zhang[a*]

a. Femtosecond Laser Laboratory, College of Physics, Jilin University, Changchun 130012, China
b. Quantum Enginerring Center, Beingjing Institute of Control Device, Beijing 100854, China
c. State Key Laboratory of Supramolecular Structure and Materials, Jilin University, Changchun 130012, China
d. State Key Laboratory of Inorganic Synthesis and Preparative Chemistry, Jilin University, Changchun 130012, China
e. Department of Physics, Harbin Institute of Technique, Harbin 150000, China

(Dated: Received on February 20, 2014; Accepted on April 28, 2014)

The optical properties of three linear conjugated oligomers (F-P, F-P-F, and P-F-P-F-P), where phenothiazine (P) and fluorene (F) groups arrange alternately, are investigated. With the enhancement of the π-conjugated system, their absorption and emission bands both gradually red shift, and their two-photon properties are also improved. Meanwhile, their fluorescence dynamic traces are analyzed with continuous rate distribution model, exhibiting that their decay rates gradually accelerate and the rate distribution width become narrower. The quantum chemical calculation offers their molecular structures and transition mechanism, showing that the enhancement of π-conjugated system should be responsible for the improvement of two-photon properties.

Key words: Oligomer, Z-scan, Fluorescence dynamics

I. INTRODUCTION

Currently, there are intense research efforts focusing on organic materials with large nonlinear optical properties, especially the two-photon absorption (TPA) properties [1], because of their huge potential applications in many extensive aspects, such as photodynamic therapy [2−4], optical storage [5], optical limiting [6−8], 3D micro-fabrication [9, 10], and two-photon fluorescence microscopy [11], *etc.* Abundant experimental and theoretical studies have been carried out to investigate the strategies for property-structure relationship of organic molecules with large TPA cross-section. According to available results, a conclusion can be drawn that electron-donor (D) and electron-acceptor (A) joined through a π-bridge to form a linear symmetrical (D-π-D or A-π-A) or asymmetrical (D-π-A) systems, which can effectively improve TPA activities [12−14]. In addition, the donor-acceptor strength, conjugation length, and nature of materials play an important role in two-photon absorption properties. Constructing a linear structure is one of the most common approaches, which could build molecules with TPA activities [15, 16]. Fluorene and phenothiazine acting as typical functional units have a large rigid structure and π-conjugated system [17]. Fluorene unit has low ionization potential which could be used as the electron donor, and the phenothiazine group owns special spatial structure and is able to restrain the aggregation owing to the π-π interaction.

In this work, we investigate the optical properties of three novel linear oligomers, in which fluorene (F) and phenothiazine (P) groups arrange alternately and the phenothiazine unit acts as the center group (F-P, F-P-F, and P-F-P-F-P, as seen in Fig.1). Z-scan measurements have been carried out on the oligomers, which offer the TPA cross-section, and the fluorescence relaxation processes of these oligomers are detected and analyzed using continuous decay rate distribution model. The quantum chemical calculations offer the molecular structures and analyze the structure-dependent electronic transition mechanisms, which exhibit that the improvement of TPA should be assigned to the enhancement of π-conjugated system in oligomers.

II. EXPERIMENTS

The fluorine-based phenothiazine oligomers (F-P, F-P-F, and P-F-P-F-P) were obtained from Lu groups at department of chemistry of Jilin university. We prepared oligomers toluene solutions with concentrations at 2.5×10^{-5} and 5.0×10^{-4} mol/L for linear and non-

*Authors to whom correspondence should be addressed. E-mail: songyunfei@hit.edu.cn, yinghui wang@jlu.edu.cn, zhanghz@jlu.edu.cn

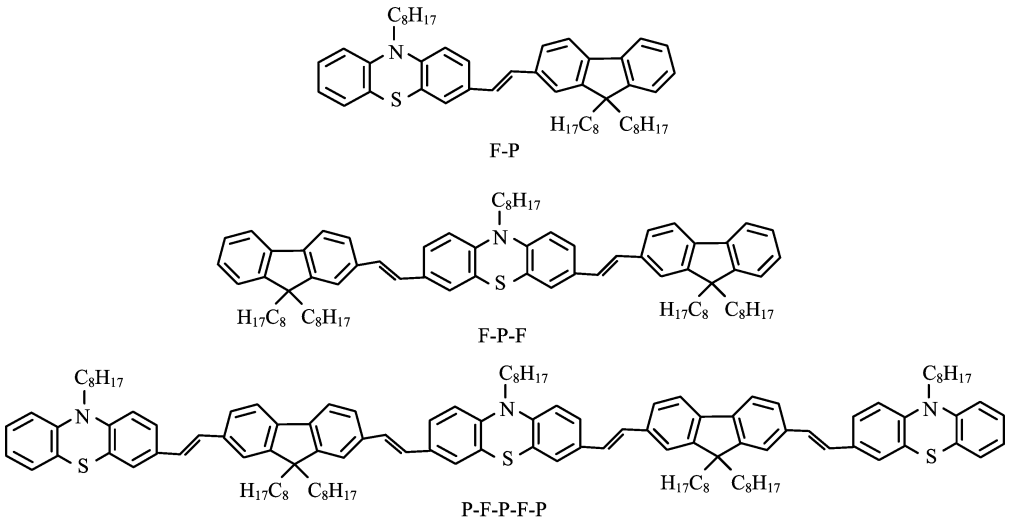

FIG. 1 Molecular structures of F-P, F-P-F, and P-F-P-F-P.

linear optical measurements, respectively. The samples were placed in a 2 mm thick quartz cuvette during the optical measurement.

Steady absorption measurements were carried out in UV-Vis absorption spectrometer (Purkinje, TU-1810PC). Femtosecond Titanium:Sapphire laser (Coherent) was used as radiation source, which offers 2.2 mJ, 130 fs pulses at 800 nm with a repetition rate of 1 kHz. One or two-photon fluorescence measurements were achieved by using CCD detector (Ocean Optics, USB4000). TPA measurements were carried out by employing the femtosecond open aperture Z-scan technique, and the laser beam was modulated by means of a mechanical chopper (∼500 Hz). The Z-scan signal passes through a lock-in amplifier and is finally detected by PMT (Zolix). TPA cross-section can be obtained through the expression

$$\sigma^{(2)} = h\nu\beta/N \tag{1}$$

where N is the number of molecule per cm^3, β is the two-photon absorption coefficient, and $h\nu$ is the photon energy. $\sigma^{(2)}$ is expressed in Goppert-Mayer units (GM), with 1 GM=1×10^{-50} cm^4s/(molecule photon).

For the emission dynamic investigations, a picoseconds laser system (Becker & Hickl GmbH, BDL-375-SMC) with a repetition rate of 20 MHz was employed to excite samples. The photoluminescence originated from samples was passed through monochromator (Zolix, SSM101) and detected by single photon detection module (id Quantique, id100-50), which was connected with TCSPC measurement card (Becker & Hickl GmbH, SPC-130) in personal computer.

III. COMPUTATIONAL METHODS

All quantum chemical calculations were done with Gaussian 09 program package [18]. The ground state geometries of F-P, F-P-F, and P-F-P-F-P were optimized with density functional theory (DFT) [19], B3LYP functional [20] and 6-31G(d) basis set. Electronic transition in optical absorption was computed with time-dependent DFT (TD-DFT) [21] using B3LYP functional and 6-31G(d) basis set. In the calculations, the side chains of oligomers were replaced by CH_3, since the influence of peripheral carbon chains was believed to be so small that they could be neglected in our quantum chemical calculations. All the electronic properties and geometries were calculated by assuming F-P, F-P-F, and P-F-P-F-P to be isolated molecules in vacuum.

IV. RESULTS AND DISCUSSION

As shown in Fig.2, the absorption spectra of F-P, F-P-F, and P-F-P-F-P in toluene (2.5×10^{-5} mol/L) show similar structures, which all have two absorption bands. With the increasing of π-conjugated units, the absorption and the one photon fluorescence (OPF) maximum of these oligomers gradually red shift (λ_{abs}: 395 nm (F-P), 410 nm (F-P-F), and 428 nm (P-F-P-F-P); λ_{em}: 500 nm (F-P), 514 nm (F-P-F), 520 nm (P-F-P-F-P)), and the corresponding light harvesting capability was also enhanced step by step.

We observe the fluorescence emission of these oligomers under the excitation of femtosecond pulses at 800 nm, and the corresponding normalized emission spectra are shown in Fig.3(a). Figure 3(b) shows that the integral emission intensity increases linearly with the increase of the square of the pump energy, which confirms that TPA is the main excitation mechanism of the intense fluorescence emission for all oligomers. In comparison with OPF spectra, the TPF shows a little difference, which mainly originates from the re-absorption effect. The slope of TPF comes from the

DOI:10.1063/1674-0068/27/03/315-320

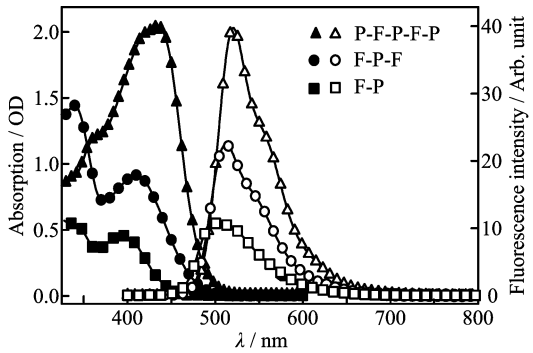

FIG. 2 Steady-state absorption (solid symbols) and one-photon induced fluorescence (open symbols) spectra of F-P, F-P-F, and P-F-P-F-P with concentration of 2.5×10^{-5} mol/L.

contribution of TPF efficiency. Apparently, the TPF efficiency of F-P increases a little in comparison with that of F-P-F. However, when two phenothiazine groups are introduced into F-P-F, the TPF efficiency apparently increases about 10 times. The open aperture Z-scan traces of F-P, F-P-F, and P-F-P-F-P are shown in Fig.3(c), which exhibits similar Z-scan curves. We firstly eliminate perturbation of toluene solvent, so that we could assess the possible contribution of the solvent nonlinearity. The nonlinear absorption coefficient β can be measured by fitting the experimental data with [22]:

$$T(z, S=1) = \sum_{m=0}^{\infty} \frac{[-q_0(z,0)]^m}{(m+1)^{3/2}} \tag{2}$$

$$q_0(z) = \frac{\beta I_0}{1 + z^2/{z_0}^2} \tag{3}$$

$$L_{\text{eff}} = 1 - \frac{\exp(-\alpha L)}{\alpha} \tag{4}$$

where T is the normalized transmittance for the open aperture Z-scan curve, L_{eff} is the effective thickness of the sample with the sample length L, α is the linear absorption coefficient, $z_0{=}k{w_0}^2/2$ is the Rayleigh length, $k{=}2\pi/\lambda$ is the wave vector, w_0 is beam waist radius of Gaussian pulse, I_0 is the pulse irradiance. The values obtained for the TPA cross-sections are summarized in Table I. Apparently, the enhancement tendency of TPA is similar to that of TPF efficiency, and the introduction of π-conjugated groups leads to the apparent enhancement of TPA cross-section.

In order to further compare the optical properties of F-P, F-P-F, and P-F-P-F-P, we present their fluorescence dynamic traces in Fig.4(a). Generally speaking, the excited level and the ground level of oligomers all consist of a ladder of sublevels. After excitation, the luminescent species quickly relax to the lowest excited electronic level on the ultrafast time scale. From this level, fluorescent transitions occur to different sublevels of the ground electronic level and each of them may relax with a certain rate. The total fluorescence decay trace should be the superposition of these dynamic processes with different rates, which makes the total fluorescence trace own a rate-distribution and shows non-exponential relaxation behaviors. In order to further analyze the structure-dependent fluorescence decay characteristics, all the fluorescence decay traces are fitted with a continuous distribution function of decay rates [23]:

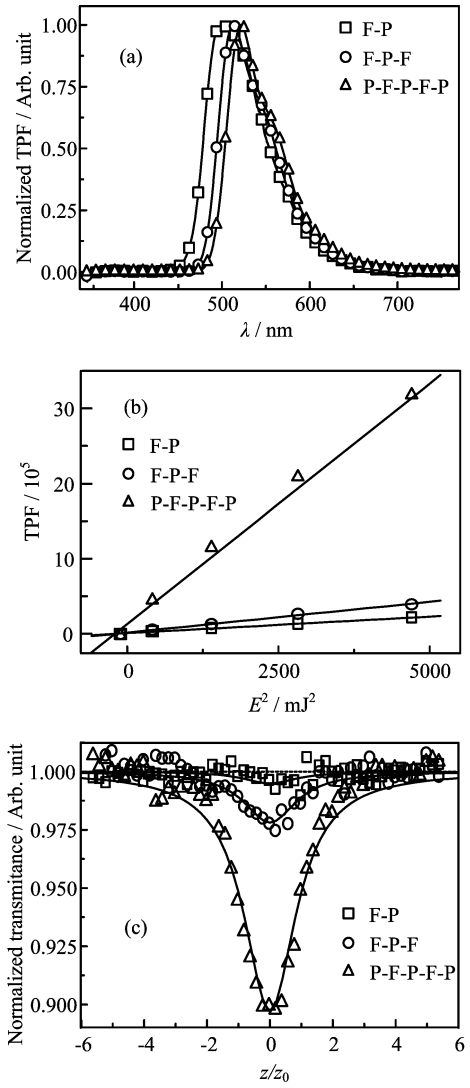

FIG. 3 (a) Normalized TPF spectra of F-P, F-P-F, and P-F-P-F-P. (b) TPF integral intensities of F-P, F-P-F, and P-F-P-F-P as a function of the square of the laser energy. π-conjugated unit dependence of normalized TPF efficiency ψ_n/ψ_1. Open aperture Z-scan curves are measured at 800 nm and the solid lines represent fittings used to extract β value. (c) Open aperture Z-scan signatures for F-P, F-P-F, and P-F-P-F-P with concentration of 5×10^{-4} mol/L (energy of pulse: ∼245 nJ).

$$I(t) = I(0) \int_{\gamma=0}^{\infty} \varphi(\gamma) \exp(-\gamma t)\, \mathrm{d}\gamma \tag{5}$$

DOI:10.1063/1674-0068/27/03/315-320

TABLE I Calculated DFT energy levels of frontier orbitals, E_g (HOMO-LUMO band gap), TPA characteristics, and dynamic fitted results of F-P, F-P-F, and P-F-P-F-P.

Compound	LUMO/eV	HOMO/eV	E_g/eV	$\beta^{(2)}$/(cm/GW)	$\sigma_E^{(2)}$/GM	γ_{MF}/ns^{-1}	$\Delta\gamma$/ns^{-1}
F-P	−1.460	−4.865	3.405	0.0015	124	0.373	0.449
F-P-F	−1.582	−4.772	3.190	0.0065	527	0.561	0.331
P-F-P-F-P	−1.749	−4.682	2.933	0.0305	2519	0.664	0.140
F	−1.125	−5.504	4.379				
P	−0.223	−5.061	4.838				

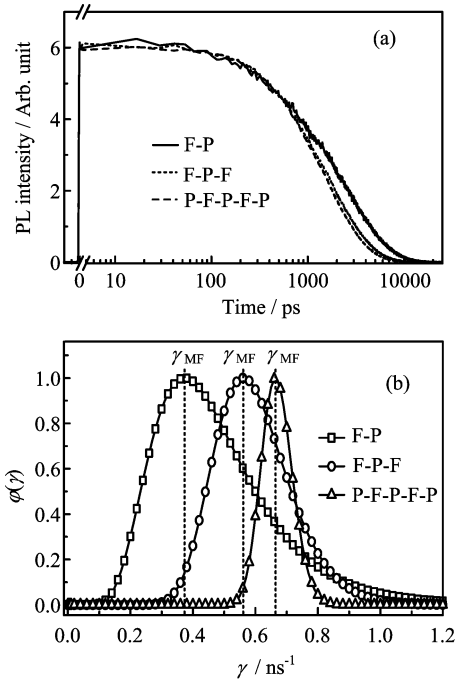

FIG. 4 (a) Fluorescence decay curves are recorded at λ_{max}=503 nm (F-P), 512 nm (F-P-F), and 520 nm (P-F-P-F-P). (b) The corresponding decay-rate distributions for the three oligomers. γ_{MF} of F-P, F-P-F, and P-F-P-F-P are 0.373, 0.561, and 0.664 ns^{-1}, and the width ($\Delta\gamma$) of their distribution function are 0.449, 0.331, 0.140 ns^{-1}.

where $\varphi(\gamma)$ is a distribution of decay rates with dimension of time, $I(t)$ is the fluoresecence intensity, $\varphi(\gamma)$ describes a distribution of the concentration of emitters with a certain γ, weighted by the corresponding γ_{rad} [24]. $\varphi(\gamma)$ is the long-normal distribution function as described below:

$$\varphi(\gamma) = A\exp\left[-\ln^2\left(\frac{\gamma/\gamma_{MF}}{w^2}\right)\right] \tag{6}$$

where γ_{MF} is the most-frequency decay rate corresponding to the maximum of $\varphi(t)$, w is a dimensionless width parameter that determines the distribution width ($\Delta\gamma$) at $1/e$, A is the normalization constant, so that

$$\int \varphi(\gamma)\mathrm{d}\gamma = 1 \tag{7}$$

The fitted lines are shown in Fig.4(a) with solid lines and the corresponding rate-distribution functions are summarized in Fig.4(b). Apparently, γ_{MF} obviously accelerates from 0.373 ns^{-1} to 0.664 ns^{-1} as the increasing of π-conjugated units in oligomers, which is in agreement with our previous report [25]. Meanwhile, the distribution width could be calculated as described below:

$$\Delta\gamma = 2\gamma_{MF}\sinh w \tag{8}$$

As seen in Fig.4(b), $\Delta\gamma$ gradually becomes narrower and decreases from 0.449 ns^{-1} to 0.140 ns^{-1}, indicating that the decay rate distribution gradually converges with the prolonging of π-conjugated length, which make the difference among decay dynamic processes becomes less and less. Meanwhile, the width of rate distribution becomes gradually narrower, indicating that the emission relaxation behavior of these conjugated materials becomes simple.

The molecular structures of F-P, F-P-F, and P-F-P-F-P in the ground state have been optimized by using B3LYP/6-31G, where the phenothiazine unit owns coplanarity, but fluorene unit does not. The molecular frontier orbitals, involving highest occupied molecular orbital (HOMO) and lowest unoccupied molecular orbital (LUMO) of F-P, F-P-F, and P-F-P-F-P are shown in Fig.5(a). After photoexcitation, the intramolecular charge transfer (ICT) doesn't occur in the F-P, F-P-F, and P-F-P-F-P oligomers, indicating that the improvement of TPA should be independent of the ICT process. The calculated HOMO and LUMO of F, P, F-P, F-P-F, and P-F-P-F-P are also offered in Fig.5(b) and summarized in Table I. Apparently, the LUMO and HOMO of F-P could be determined by LUMO of F and HOMO of P groups, respectively. After the F and P groups alternatively linking on the F-P oligomer, the energy level of HOMO would gradually decrease and that of LUMO would increase step by step. With the narrowing of band gap of oligomers, the absorption maximum of oligomers should red shift, which is in agreement with the experimental data as seen in Fig.2.

In addition, we also calculated the absorption spectra of F-P, F-P-F, and P-F-P-F-P, as shown in Fig.6. It is noted that the absorption band edge of oligomers gradually red shifts with the increasing of π-conjugated groups, which is in agreement with the experimental

DOI:10.1063/1674-0068/27/03/315-320

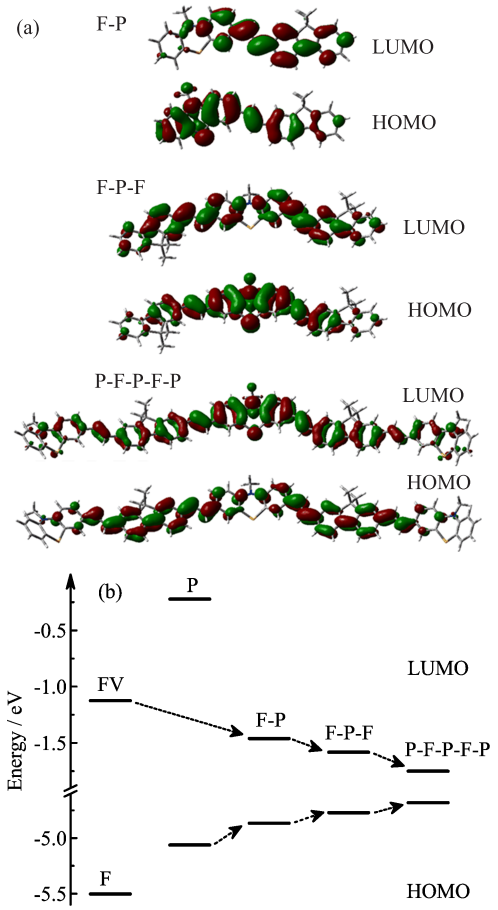

FIG. 5 (a) HOMO and LUMO of F-P, F-P-F, and P-F-P-F-P with the B3LYP method and (b) the corresponding energy level of them.

data. Moreover, the calculated spectra of F-P, F-P-F, and P-F-P-F-P all have two main absorption bands, which are also similar to the experimental data. The calculated electronic transition is assumed to be in the vacuum, therefore there is a little difference between the theoretical and experimental data. As seen in Table II, the contribution of the frontier molecular orbitals to electronic transitions of three oligomers are analyzed in detail. The main absorption bands of three oligomers are all ascribed to $S_0 \rightarrow S_1$ transition, which is mainly composed of HOMO→LUMO transition. Apparently, the $S_0 \rightarrow S_1$ transition almost has no intramolecular charge transfer character, which is not able to influence the two photon absorption properties. The improvement of TPA should be assigned to the enhancement of π-conjugated system.

V. CONCLUSION

The optical properties of three linear conjugated oligomers (F-P, F-P-F, and P-F-P-F-P) are investigated in detail. Steady-state spectral measurements

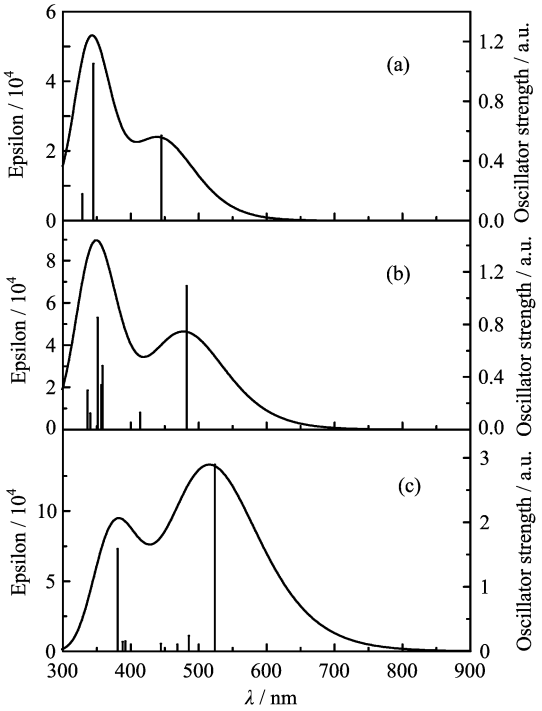

FIG. 6 Calculated absorption spectra of (a) F-P, (b) F-P-F, and (c) P-F-P-F-P.

show that the absorption and emission bands of these oligomers all red shift with the enhancement of π-conjugated system and other optical properties are all modulated. Two-photon fluorescence and femtosecond open aperture Z-scan techniques confirm that the two-photon fluorescence yield and the two-photon absorption cross-section of these oligomers all also enhance with the improvement of π-conjugated system. Time-resolved fluorescence measurements exhibit that the relaxation process gradually accelerates and the fitted results based on continuous decay rate distribution model exhibits that the decay rate of oligomers gradually accelerate and the distribution width become narrower and narrower from F-P to P-F-P-F-P. The quantum chemical calculations offer the molecular structures and analyze the electronic transition mechanisms, which point out that the improvement of TPA properties should depend on the enhancement of π-conjugated system. All the results could be much useful for us to further understand the photophysical properties of linear oligomers.

VI. ACKNOWLEDGMENTS

This work was supported by the National Natural Science Foundation of China (No.21103161, No.11274142, No.11304058, No.11274034, and No.11004080) and the China Postdoctoral Science Foundation (No.2011M500927 and No.2013T60319).

DOI:10.1063/1674-0068/27/03/315-320

TABLE II Calculated transition energies E and oscillator strengths f for F-P, F-P-F and P-F-P-F-P.

	Transition state	E/nm(eV)	f	Major contribution
F-P	S_1	445.17(2.78)	0.5688	H→L (95%)
	S_3	344.86(3.59)	1.0518	H-1→L (87%)
	S_5	328.61(3.77)	0.1773	H→L+1 (13%), H→L+2 (34%), H→L+3 (17%), H→L+4 (24%)
F-P-F	S_1	482.30(2.57)	1.0931	H→L (97%)
	S_3	358.37(3.45)	0.4843	H-2→L (59%), H-1→L (18%)
	S_4	356.47(3.47)	0.3399	H-1→L (35%), H→L+2 (17%), H→L+3 (10%), H→L+4 (25%)
	S_5	351.04(3.53)	0.8510	H-2→L (28%), H-1→L (41%), H→L+2 (14%)
	S_7	336.38(3.69)	0.2979	H-1→L+1 (48%), H→L+2 (30%)
P-F-P-F-P	S_1	523.69(2.36)	2.8958	H→L (72%)
	S_2	485.52(2.55)	0.2414	H-1→L (58%), H→L+1 (28%)
	S_9	391.95(3.16)	0.1561	H-3→L (10%), H-2→L+2 (42%), H-1→L+3 (20%)
	S_{10}	388.12(3.19)	0.1466	H-3→L (71%), H-2→L+2 (11%)
	S_{12}	380.53(3.25)	1.5873	H-4→L (47%), H-3→L+1 (39%)

[1] C. Andraud, R. Fortrie, C. Barsu, O. Stephan, H. Chermette, and P. L. Baldeck, Adv. Polym. Sci. **214**, 149 (2008).

[2] D. Gao, R. R. Agayan, H. Xu, M. A. Philbert, and R. Kopelman. Nano Lett. **6**, 2383 (2006).

[3] C. Andraud, R. Fortrie, C. Barsu, O. Stephan, H. Chermette, and P. L. Baldeck, Adv. Polym. Sci. **214**, 149 (2008).

[4] T. Francesca, K. Claudine, B. Ekaterina, T. Sergei, and B. D. Mireille, Adv. Mater. **20**, 4641 (2008).

[5] D. A. Parthenopoulos and P. M. Rentzepis, Science **245**, 843 (1989).

[6] I. Fuks-Janczarek, J. Ebothe, R. Miedzinski, R. Gabanski, A. H. Reshak, M. Lapkowski, R. Motyka, I. Kityk, and J. Suwinski, Laser Phys. **18**, 1056 (2008).

[7] M. P. Joshi, H. E. Pudavar, J. Swiatkiewicz, P. N. Prasad, and B. A. Reinhardt, Appl. Phys. Lett. **74**, 170 (1999).

[8] H. B. Sun, T. Suwa, K. Takada, R. P. Zaccaria, M. S. Kim, K. S. Lee, and S. Kawata, Appl. Phys. Lett. **83**, 1104 (2004).

[9] S. Kawata, H. B. Sun, T. Tanaka, and K. Takada, Nature **412**, 697 (2001).

[10] W. Zhou, S. M. Kuebler, K. L. Brauo, T. Yu, J. K. Cammack, C. K. Ober, J. W. Perry, and S. R. Marder, Science **296**, 1106 (2002).

[11] M. C. Skala, J. M. Squirrell, K. M. Vrotsos, V. C. Eickhoff, A. Gendron-Fitzpatrick, K. W. Eliceiri, and N. Ramanujam, Cancer Res. **65**, 1180 (2005).

[12] G. S. He, L. S. Tan, Q. D. Zheng, and P. N. Prasad, Chem. Rev. **108**, 1245 (2008).

[13] N. Pucher, A. Rosspeintner, V. Satzinger, V. Schmidt, G. Gescheidt, J. Stampfl, and R. Liska, Macromolecules **42**, 6519 (2009).

[14] Z. Q. Li, M. Siklos, N. Pucher, K. Cicha, A. Ajami, W. Husinsky, A. Rosspeintner, E. Vauthey, G. Gescheidt, J. Stampfl, and R. Liska, J. Polym. Sci. A **49**, 3688 (2011).

[15] T. H. Huang, D. Yang, Z. H. Kang, E. L. Miao, R. Lu, H. P. Zhou, F. Wang, G. W Wang, P. F. Cheng, Y. H. Wang, and H. Z. Zhang, Opt. Mater. **35**, 467 (2013).

[16] T. H. Huang, X. C. Li, Y. H. Wang, Z. H. Kang, R. Lu, E. L. Miao, F. Wang, G. W. Wang, and H. Z. Zhang, Opt. Mater. **35**, 1373 (2013).

[17] Z. H. Kang, N. Sui, Y. H. Wang, L. Zou, C. Qian, R. Lu, and H. Z. Zhang, J. Mol. Struct. **89**, 1054 (2013).

[18] M. J. Frisch, G. W. Trucks, H. B. Schlegel, G. E. Scuseria, M. A. Robb, J. R. Cheeseman, G. Scalmani, V. Barone, B. Mennacci, G. A. Peterson, H. Nakatsuji, M. Caricato, X. Li, H. P. Hratchian, A. F. Izmaylov, J. Bloino, G. Zheng, J. L. Sonnenberg, M. Hada, M. Ehara, K. Toyota, R. Fukuda, J. Hasegawa, M. Ishida, T. Nakajima, Y. Honda, O. Kitao, H. Nakai, T. Vreven, J. A. Jr. Montgomery, J. E. Peralta, F. Ogliaro, M. Bearpark, J. J. Heyd, E. Brothers, K. N. Kudin, V. N. Staroverov, R. Kobayashi, J. Normand, K. Raghavachari, A. Rendell, J. C. Burant, S. S. Iyengar, J. Tomasi, M. Cossi, N. Rega, J. M. Millam, M. Klene, J. E. Knox, J. B. Cross, V. Bakken, C. Adamo, J. Jaramillo, R. Gomperts, R. E. Stratmann, O. Yazyev, A. J. Austin, R. Cammi, C. Pomelli, J. W. Ochterski, R. L. Martin, K. Morokuma, V. G. Zakrzewski, G. A. Voth, P. Salvador, J. J. Dannenberg, S. Dapprich, A. D. Daniels, Ö. Farkas, J. B. Foresman, J. V. Ortiz, J. Cioslowski, and D. J. Fox, *Gaussian 09, Revision A.02*, Wallingford CT: Gassian, Inc., (2009).

[19] P. Hohenberg and W. Kohn, Phys. Rev. **136**, B864 (1964).

[20] A. D. Becke, Phys. Rev. A **38**, 3098 (1988).

[21] E. K. U. Gross and W. Kohn, Phys. Rev. Lett. **55**, 2850 (1985).

[22] M. Sheik-Bahae, A. A. Said, T. H. Wei, D. J. Hagan, and E. W. van Stryland, IEEE J. Quantum Electron. **26**, 760 (1990).

[23] I. S. Nikolaev, P. Lodahl, A. F. van Driel, A. F. Koenderink, and W. L. Vos, Phys. Rev. B **75**, 115302 (2007).

[24] A. F. van Driel, I. S. Nikolaev, P. Vergeer, P. Lodahl, D. Vanmakekelbergh, and W. L. Vos, Phys. Rev. B **75**, 035329 (2007).

[25] L. J. Gong, Y. H. Wang, Z. H. Kang, T. H. Huang, R. Lu, and H. Z. Zhang, Chin. J. Chem. Phys. **25**, 636 (2012).

DOI:10.1063/1674-0068/27/03/315-320